Materials and Design 87 (2015) 540–552

Contents lists available at ScienceDirect

Materials and Design

journal homepage: www.elsevier.com/locate/jmad

Description of stress–strain curves for stainless steel alloys

I. Arrayago [a,*], E. Real [a], L. Gardner [b]

[a] Department of Construction Engineering, Jordi Girona 1-3, Universitat Politècnica de Catalunya, Barcelona 08034, Spain
[b] Department of Civil Engineering, Skempton Building, South Kensington Campus, Imperial College London, London SW7 2AZ, UK

ARTICLE INFO

Article history:
Received 6 November 2014
Received in revised form 28 July 2015
Accepted 1 August 2015
Available online 5 August 2015

Keywords:
Constitutive law
Material modelling
Nonlinear stress–strain behaviour
Stress–strain curves
Stainless steel
Tensile tests

ABSTRACT

There is a wide variety of stainless steel alloys, but all are characterized by a rounded stress–strain response with no sharply defined yield point. This behaviour can be represented analytically by different material models, the most popular of which are based on the Ramberg–Osgood formulations or extensions thereof. The degree of roundedness, the level of strain hardening, the strain at ultimate stress and the ductility at fracture of the material all vary between grades, and need to be suitably captured for an accurate representation of the material to be achieved. The aim of the present study is to provide values and predictive expressions for the key parameters in existing stainless steel material models based on the analysis of a comprehensive experimental database. The database comprises experimental stress–strain curves collected from the literature, supplemented by some tensile tests on austenitic, ferritic and duplex stainless steel coupons conducted herein. It covers a range of stainless steel alloys, annealed and cold-worked material, and data from the rolling and transverse directions. In total, more than 600 measured stress–strain curves have been collected from 15 international research groups. Each curve from the database has been analysed in order to obtain the key material parameters through a curve fitting process based on least squares adjustment techniques. These parameter values have been compared to those calculated from existing predictive models, the accuracy of which could therefore be evaluated. Revised expressions providing more accurate parameter predictions have been proposed where necessary. Finally, a second set of results, containing material parameters reported directly by others, with information of more than 400 specimens, has also been collected from the literature. Although these experimental results were not accessible as measured raw data, they enabled further confirmation of the suitability of the proposed equations.

1. Introduction

Stainless steel is gaining increasingly widespread usage in a range of engineering applications. The material is characterized by a nonlinear stress–strain curve which differs from that typically exhibited by hot-finished carbon steel, but shows similarities with other construction materials such as cold-worked steel and aluminium. Different material models describing this nonlinear stress–strain behaviour have been developed in the last few decades, the most widely used of which are based on the expression originally proposed by Ramberg and Osgood [1] and modified by Hill [2]. An accurate description of the stress–strain behaviour of stainless steel is essential for use in structural design codes, and advanced analytical and numerical models, whose applications may include the simulation of section forming, the structural behaviour of members and connections, the response of structures under extreme loads, and so on.

Existing material models require certain key material parameters to be defined. Values for these parameters can be obtained from measured stress–strain curves, but are also provided in Standards, such as EN 1993-1-4 [3] through tables and predictive expressions. However, recent research by Real et al. [4], Arrayago et al. [5] and Afshan et al. [6] has shown that the parameter values derived from EN 1993-1-4 are not always accurate. Hence, this paper presents a detailed evaluation of predictive expressions for the key material parameters, gathered both from current design codes and proposed in the literature against a comprehensive database of stainless steel stress–strain curves. A range of stainless steel grades, production routes, section types, direction of testing with respect to the rolling direction and sample thicknesses have been considered.

2. Existing material models, standards and previous work

2.1. Existing material models

The nonlinear stress–strain behaviour exhibited by the different stainless steel grades can be analytically described by various material models. The most widely used are based on the general expression originally proposed by Ramberg and Osgood [1] and modified by Hill [2], as

* Corresponding author at: C/Jordi Girona 1-3, C1 Building (207), Barcelona 08034, Spain.
E-mail addresses: itsaso.arrayago@upc.edu (I. Arrayago), esther.real@upc.edu (E. Real), leroy.gardner@imperial.ac.uk (L. Gardner).

http://dx.doi.org/10.1016/j.matdes.2015.08.001
0264-1275/

given by Eq. (1), where E is the Young's modulus, $\sigma_{0.2}$ is the 0.2% proof stress conventionally considered as the yield stress, and n is the strain hardening exponent, usually calculated from Eq. (2).

$$\varepsilon = \frac{\sigma}{E} + 0.002\left(\frac{\sigma}{\sigma_{0.2}}\right)^{n} \tag{1}$$

$$n = \frac{\ln(20)}{\ln\left(\frac{\sigma_{0.2}}{\sigma_{0.01}}\right)} \tag{2}$$

where $\sigma_{0.01}$ is the 0.01% proof stress. The basic Ramberg–Osgood formulation has been shown to be capable of accurately representing different regions of the stress–strain curve, depending on the choice of the n parameter, but to be generally incapable of accurately representing the full stress–strain curve with a single value of n. This observation led to the development of various two-stage Ramberg–Osgood models that were capable of providing a single continuous representation of the stress–strain curve of stainless steel from the onset of loading to the ultimate tensile stress. Mirambell and Real [7] proposed a two-stage model based on the Ramberg–Osgood expression, but defining a second curve for stresses above the 0.2% proof stress, with a new reference system, denoted $\sigma^* - \varepsilon^*$ and presented in Fig. 1, where the transformation of the variables to the new reference system from the original one is defined in Eqs. (3) and (4), where $\varepsilon_{0.2}$ is the total strain at the 0.2% proof stress.

$$\sigma^* = \sigma - \sigma_{0.2} \tag{3}$$

$$\varepsilon^* = \varepsilon - \varepsilon_{0.2} \tag{4}$$

Hence, the second curve can be defined as established in Eq. (5) in terms of the new $(\sigma^* - \varepsilon^*)$ reference system and according to Eq. (6) if the general $(\sigma - \varepsilon)$ system is considered, with an additional strain hardening exponent, m, for the second stage. Eq. (1) continued to apply for stresses less than or equal to the 0.2% proof stress.

$$\varepsilon^* = \frac{\sigma^*}{E_{0.2}} + \varepsilon^*_{up}\left(\frac{\sigma^*}{\sigma^*_u}\right)^{m} \quad \text{for} \quad \sigma > \sigma_{0.2} \tag{5}$$

$$\varepsilon = \frac{\sigma - \sigma_{0.2}}{E_{0.2}} + \left(\varepsilon_u - \varepsilon_{0.2} - \frac{\sigma_u - \sigma_{0.2}}{E_{0.2}}\right)\left(\frac{\sigma - \sigma_{0.2}}{\sigma_u - \sigma_{0.2}}\right)^{m} + \varepsilon_{0.2} \quad \text{for} \quad \sigma > \sigma_{0.2} \tag{6}$$

Fig. 2. Austenitic stainless steel coupons before and after testing.

where $E_{0.2}$ is the tangent modulus at the 0.2% proof stress, given by Eq. (7), σ^*_u and ε^*_{up} are the ultimate strength and ultimate plastic strain according to the new reference system, σ_u and ε_u are the ultimate strength and total strain in terms of the general system and $\varepsilon_{0.2}$ is the total strain at the 0.2% proof stress.

$$E_{0.2} = \frac{E}{1 + 0.002n\frac{E}{\sigma_{0.2}}} \tag{7}$$

Fig. 1 shows a typical stainless steel stress–strain curve where both the general $(\sigma - \varepsilon)$ and the new $(\sigma^* - \varepsilon^*)$ reference systems are plotted, together with the key symbols used in the material modelling expressions. The parameter ε_{up} is the ultimate plastic strain and ε_f is the strain at fracture, both expressed in the general reference system. The remaining symbols are as previously defined.

In order to reduce the number of required input parameters, the two-stage Ramberg–Osgood model was simplified by Rasmussen [8], leading to the revised expression for $\sigma > \sigma_{0.2}$ given by Eq. (8). This equation assumes that the ultimate plastic strain ε^*_{up} in terms of the second reference system is equal to the general ultimate total strain ε_u, as expressed in Eq. (9). Rasmussen [8] also developed predictive expressions for the determination of the second strain hardening parameter m, the ultimate strain and the ultimate strength, as given by Eqs. (10)–(12b) respectively, effectively reducing the number of required input parameters to the three basic Ramberg–Osgood parameters (E, $\sigma_{0.2}$ and n). This proposal was included in EN 1993-1-4, Annex C [3] for the modelling of stainless steel material behaviour.

$$\varepsilon = \frac{\sigma - \sigma_{0.2}}{E_{0.2}} + \varepsilon_u\left(\frac{\sigma - \sigma_{0.2}}{\sigma_u - \sigma_{0.2}}\right)^{m} + \varepsilon_{0.2} \quad \text{for} \quad \sigma > \sigma_{0.2} \tag{8}$$

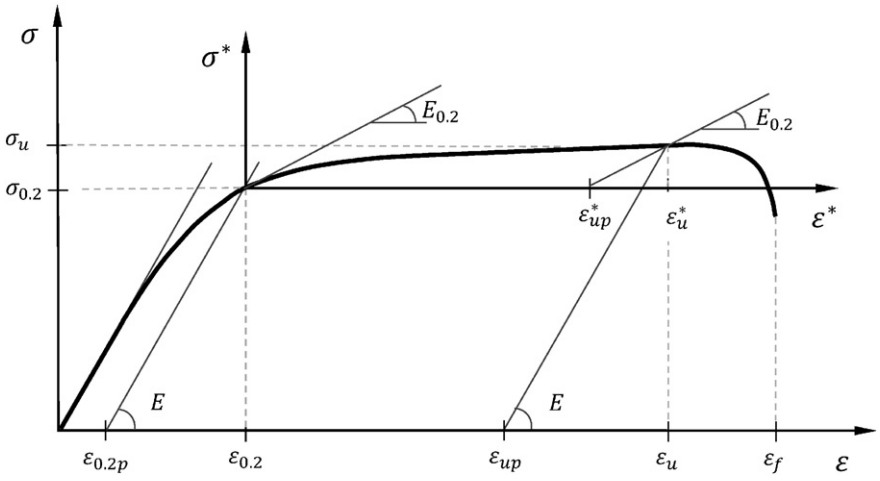

Fig. 1. Typical stress–strain curve with definitions of key material parameters.

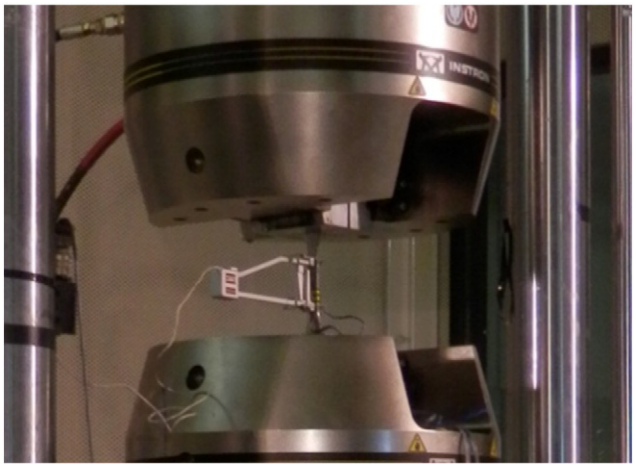

Fig. 3. Coupon in INSTRON tensile testing machine.

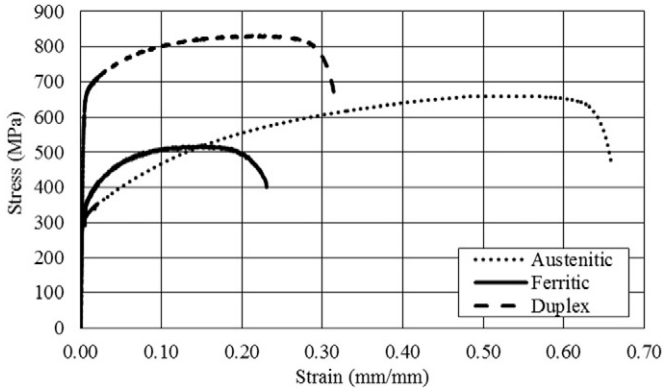

Fig. 4. Measured stress–strain curves for each of the studied stainless steel families.

$$\varepsilon^{*}_{up} = \varepsilon_u - \varepsilon_{0.2} - \frac{\sigma_u - \sigma_{0.2}}{E_{0.2}} \cong \varepsilon_u \tag{9}$$

$$m = 1 + 3.5\frac{\sigma_{0.2}}{\sigma_u} \tag{10}$$

$$\varepsilon_u = 1 - \frac{\sigma_{0.2}}{\sigma_u} \tag{11}$$

$$\frac{\sigma_{0.2}}{\sigma_u} = 0.20 + 185\frac{\sigma_{0.2}}{E} \quad \text{for austenitic and duplex stainless steels} \tag{12a}$$

$$\frac{\sigma_{0.2}}{\sigma_u} = \frac{0.20 + 185\frac{\sigma_{0.2}}{E}}{1 - 0.0375(n-5)} \quad \text{for all stainless steel alloys} \tag{12b}$$

The material model proposed by Mirambell and Real [7] was also modified by Gardner and Ashraf [9] in order to improve the accuracy of the model at low strains (less than approximately 10%) and to allow the model to be applied also to the description of compressive stress–strain behaviour. The modifications involved use of the 1% proof stress instead of the ultimate stress in the second stage of the model, leading to Eq. (13). Hence, the revised curve passes through the 1% proof stress $\sigma_{1.0}$ and corresponding total strain $\varepsilon_{1.0}$, but strains are not limited to $\varepsilon_{1.0}$ and the model provides excellent agreement with experimental stress–strain data for strains up to about 10% both in tension and compression. The second strain hardening exponent was denoted $n_{0.2,1.0}$. A further two-stage model was also proposed by Gardner et al. [10] for application to stainless steel material modelling in fire. In the proposal, the second stage of the curve passed through the stress at 2% total strain, since this strength is widely used in structural fire design.

Table 1
Average experimental material properties from reference and corroborating tests.

		E (MPa)	$\sigma_{0.1}$ (MPa)	$\sigma_{0.2}$ (MPa)	σ_u (MPa)	ε_u (%)	ε_f (%)
Reference tests (UPC)	Austenitic	207,600	280	295	668	56.1	68.2
	Ferritic	213,800	301	316	502	15.6	29.7
	Duplex	213,600	589	634	830	21.8	40.7
Corroborating tests (IC)	Austenitic	202,900	285	302	653	–	67.3
	Ferritic	213,300	303	324	520	–	27.8
	Duplex	208,800	611	652	854	–	41.3

$$\varepsilon = \frac{\sigma - \sigma_{0.2}}{E_{0.2}} + \left(\varepsilon_{1.0} - \varepsilon_{0.2} - \frac{\sigma_{1.0} - \sigma_{0.2}}{E_{0.2}}\right)\left(\frac{\sigma - \sigma_{0.2}}{\sigma_{1.0} - \sigma_{0.2}}\right)^{n_{0.2,1.0}} + \varepsilon_{0.2} \text{ for } \sigma_{0.2} < \sigma < \sigma_u \tag{13}$$

For certain modelling scenarios, such as representing cold-forming processes and connection behaviour, an accurate material description up to very high strains is often required. This requirement led to the development of three- stage versions of the Ramberg–Osgood formulation: Quach et al. [11] proposed a material model that uses the basic Ramberg–Osgood curve (Eq. (1)) for the first stage, covering stresses up to the 0.2% proof stress, the Gardner and Ashraf [9] model (Eq. (13)) for the second stage covering stresses up to the 2% proof stress and a straight line from the 2% proof stress to the ultimate strength for the third stage. More recently, Hradil et al. [12] proposed an alternative three-stage model which uses the Ramberg–Osgood equation for every stage, but with different reference systems.

The comparative study presented in [4] highlighted that three-stage models provide the most accurate fit to experimental stress–strain curves at high strains, although a high number of parameters are needed for their definition. Therefore, considering that two-stage models representing full stainless steel stress–strain curves up to σ_u [7,8] also showed excellent agreement with experimental results, it was concluded that two-stage models with a reduced number of material parameters offered the best balance between accuracy and practicality.

Fig. 5. Tensile coupon tests conducted at Imperial College London.

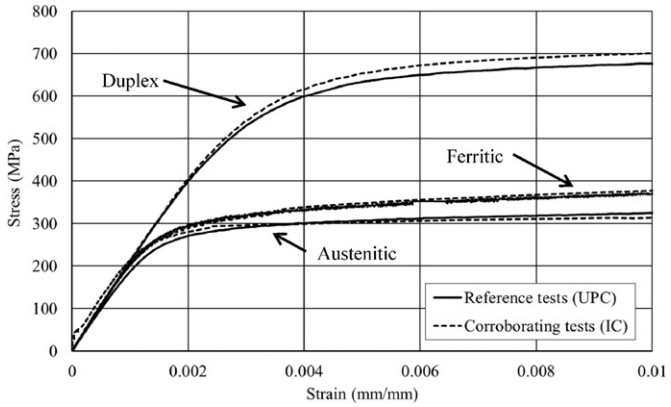

Fig. 6. Comparison of measured stress–strain curves up to 1% strain for the three stainless steel families.

2.2. EN 1993-1-4 material model and proposed modifications

The material model provided in Annex C of EN 1993-1-4 [3] for the analytical description of the stress–strain behaviour of stainless steel is based on the model proposed by Rasmussen [8] and described by Eqs. (1) and (8). The additional expressions developed by Rasmussen for the determination of some of the material parameters are also given, including Eq. (10) for the second strain hardening parameter m and Eq. (11) for the ultimate strain. The strain hardening exponent n can be obtained either from experimental data by means of Eq. (2) or from Table 2.1 of EN 1993-1-4 [3].

Recent studies (Real et al. [4], Arrayago et al. [5], Afshan et al. [6]) have confirmed the general accuracy of the form of the EN 1993-1-4 material model, but have identified some limitations in the predictive expressions for the key material parameters. These are highlighted in the present paper.

Table 3
Number of curves considered in the different analyses for Database I.

	Group I	Group II
Austenitic	367	171
Ferritic	126	94
Duplex and lean duplex	110	50
Total	603	315

3. Experimental data: tests and collection

In this section, experimental data are collected in order to evaluate the predictive models for the key material parameters given in Annex C of EN 1993-1-4, and to provide revised proposals in instances where shortcomings are identified. Additional stress–strain data are also generated herein, as described in Sections 3.1 and 3.2.

3.1. Tensile coupon tests

Tensile coupon tests were conducted on selected stainless steel grades in order to supplement the existing database of results. The coupons were cut from sheet material and tested in the rolling direction at the Universitat Politècnica de Catalunya (UPC). A total of 42 tensile tests were conducted; 14 on austenitic grade 1.4301 material, 14 on ferritic grade 1.4016 material and 14 on duplex grade 1.4462 material. Material properties, including Young's modulus E, various proof stresses ($\sigma_{0.01}$, $\sigma_{0.05}$, $\sigma_{0.2}$ and $\sigma_{1.0}$), the ultimate tensile stress σ_u, the corresponding strain ε_u and the strain at fracture ε_f, measured over the standard

Table 2
Summary of assembled experimental stress–strain curves (Database I).

Family	Grade	No. of curves	Product type	RD/TD/45°	T/C	Thickness range (mm)	Reference
Austenitic	1.4301	14	Sheet	RD	T	3	Current paper
	1.4301	6	Sheet	RD	T	4–8	Estrada et al. [15]*
							Real et al. [16]*
	1.4301, 1.4435, 1.4541, 1.4307	18	Sheet	RD	T	1–3	Outokumpu*
	1.4301	8	Cold-formed	RD	T	3–4	Nip et al. [17]
	1.4301	9	Sheet	RD	T	2–5	Xu and Szalyga [18]
	1.4301, 1.4571, 1.4404	42	Cold-formed	RD	T	2–8	Afshan et al. [6]
	1.4301	59	Cold-formed	RD	T	2–8	Gardner [19]
							Gardner and Nethercot [20]
	1.4301	57	Cold-formed, sheet	RD	C	2–8	Gardner [19]
							Gardner and Nethercot [20]
	1.4301	52	Cold-formed	RD	T	2–6	Talja [21–23]
	1.4318, 1.4301	87	Cold-formed	RD	T	3	Talja [24]
	1.4301	8	Cold-formed	RD	T	2–5	Zhou and Young [25]
	HSA	4	Cold-formed	RD	T	2–5	Zhou and Young [25]
Ferritic	1.4016	15	Sheet	RD	T	3	Current paper
	1.4003, 1.4016, 1.4509, 1.4521	30	Sheet	RD	T	1.5–3.5	Manninen [26]*
	1.4003, 1.4016, 1.4509, 1.4521	27	Sheet	TD	T	1.5–3.5	Manninen [26]
	1.4003	10	Cold-formed, sheet	RD	T	0.8	Real et al. [27]
	1.4003, 1.4509	20	Cold-formed	RD	T	3	Afshan and Gardner [28]
	1.4003, 1.4509	14	Cold-formed	RD	T	2–8	Afshan et al. [6]
	1.4003	9	Sheet	RD, TD, 45°	T	1.5	Rossi [29]
	1.4509	21	Cold-formed	RD	T	1–3	Talja and Hradil [30]
Duplex and lean duplex	1.4462	14	Sheet	RD	T	3	Current paper
	1.4462	7	Cold-formed	RD	T	2–8	Afshan et al. [6]
	1.4462	6	Cold-formed	RD	T	2–6	Talja [21]
	1.4462	5	Cold-formed	RD	T	2–5	Zhou and Young [25]
	1.4162	18	Cold-formed	RD	T	3–4	Theofanous and Gardner [31]
	1.4162	25	Sheet	RD, TD	T, C	4–20	Saliba and Gardner [32]
	1.4162	23	Sheet	RD, TD	T, C	6–12	Saliba and Gardner [33]
	1.4162	12	Cold-formed	RD	T	1.5–2.5	Huang and Young [34]

*: experimental curves included in Real et al. [4].
RD: rolling direction, TD: transverse direction, 45°: 45° from the rolling direction.
T: tension, C: compression.
HSA: high strength austenitic.

Table 4
Assessment of Eq. (9) for the different stainless steel families.

	ε_u (mm/mm)	$\varepsilon_{0.2}+\frac{\sigma_u-\sigma_{0.2}}{E_{0.2}}$ (mm/mm)	$\frac{1}{\varepsilon_u}(\varepsilon_u+\varepsilon_{0.2}+\frac{\sigma_u-\sigma_{0.2}}{E_{0.2}})$		
	Mean	Mean	Mean	Min	Max
Austenitic	0.42	0.018	1.04	1.02	1.08
Ferritic	0.13	0.015	1.20	1.02	1.81
Duplex and lean duplex	0.20	0.012	1.05	1.03	1.19

gauge length of $5.65\sqrt{A_c}$ where A_c is the cross-sectional area of the coupon, were recorded.

All tested coupons had a nominal thickness of 3 mm and a nominal width of 12 mm in the necked region. A gauge length of 50 mm was adopted in accordance with ISO 6892-1 [13]. Fig. 2 shows a typical coupon prior to and subsequent to testing. The tensile tests were conducted under strain control in an INSTRON 8805 500 kN machine. The strain rates were defined in accordance with ISO 6892-1 [13]: 0.1 mm/min for the initial part of the tests, up to approximately 1% strain increasing to 2.2 mm/min thereafter.

The longitudinal strain was measured using an MTS extensometer with two contact points, and was mounted directly onto the coupons (see Fig. 3). Two additional linear electrical resistance strain gauges were attached to the centre part of each specimen, in order to ensure an accurate measurement of the Young's modulus and to confirm the data obtained from the extensometer in the initial part of the tests.

The mean values of the key measured material parameters for the different studied stainless steel grades are reported in Table 1. An example of a measured stress–strain curve for each of the tested stainless steel grades is shown in Fig. 4. Further details of the tensile coupon tests and results are reported in Arrayago et al. [5].

For some of the specimens, repeated coupon tests were performed, for corroboration purposes, at Imperial College London (IC). These tests were carried out in a 150 kN INSTRON machine, shown in Fig. 5, under displacement control and using similar testing procedures to those described above. The reference (UPC) and corroborating (IC) test results are compared in Table 1 and Fig. 6, where a maximum discrepancy between the measured strengths of less than 3% may be observed. The influence of the testing machine may therefore be considered to be small. Similar conclusions were reached by Huang and Young [14] in recent research.

3.2. Additional data collected from the literature

In previous recent studies conducted by the authors (Real et al. [4], Arrayago et al. [5] and Afshan et al. [6]) experimental stress–strain data on austenitic, ferritic and duplex stainless steel material were generated and preliminary assessments of the material modelling

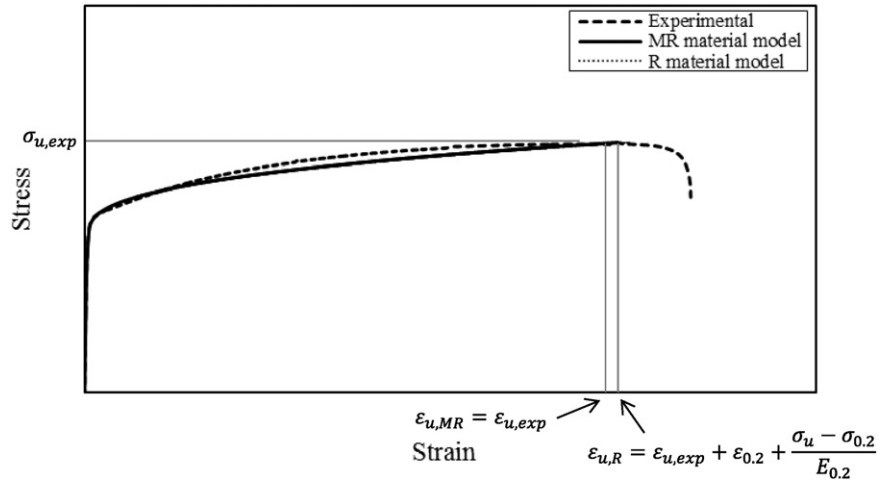

Fig. 7. Comparison of Mirambell–Real (MR) and Rasmussen (R) material models with an experimental austenitic stainless steel stress–strain curve.

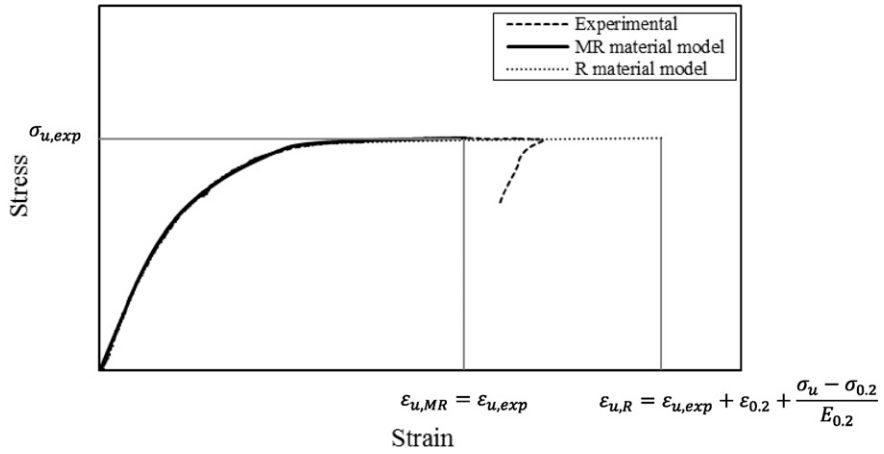

Fig. 8. Comparison of Mirambell–Real (MR) and Rasmussen (R) material models with an experimental ferritic stainless steel stress–strain curve.

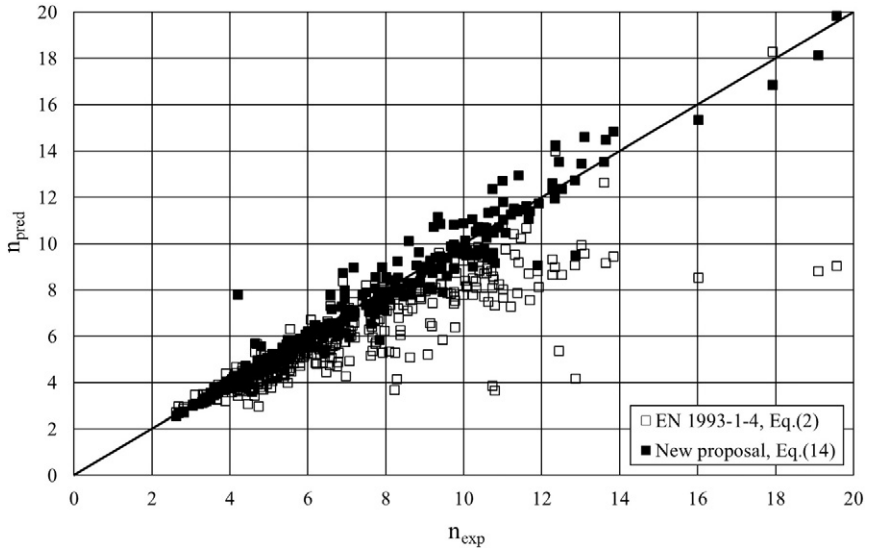

Fig. 9. Prediction of strain hardening parameter *n* for austenitic stainless steels.

provisions of EN 1993-1-4 were made. The need for further work was also highlighted. Hence, in order to enable an extensive analysis of the current provisions, a comprehensive database of experimental results has been assembled from the literature. The database, referred to as Database I in the paper to differentiate it from a second database introduced later, consists of more than six hundred measured stress–strain curves, supplied as raw data by international research groups, and covers a range of stainless steel grades and products. Note that the majority of the collected results were from coupons tested in the rolling direction (RD) but a limited number were tested in the transverse and 45° directions (TD and 45° respectively); both tensile (T) and compressive (C) behaviour of the material was also considered. A summary of the assembled results is given in Table 2. Note also that when "cold-formed" is specified as the type of material in Table 2, this covers both flat and corner coupons extracted from cold-formed sections.

4. Analysis of results and recommendations

The aforementioned data are analysed in this section in order to obtain the key material and strain hardening parameters for different stainless steel families and material types, after which the accuracy of the different expressions set out in EN 1993-1-4 and proposed in previous research for the determination of the key parameters, is assessed.

4.1. Analysis approach

Full stress–strain curves were not available for all the supplied data, since in some cases only strain gauge measurements up to about 1% strain were provided. For the calculation of the material parameters related to the initial part of the stress–strain behaviour (i.e., Young's modulus E, first strain hardening exponent *n* and initial proof stresses $\sigma_{0.01}$, $\sigma_{0.05}$, $\sigma_{0.2}$), all the collected curves (denoted Group I) have been analysed. However, when the ultimate characteristics of the material (i.e., second strain hardening parameter *m*, ultimate strain ε_u, ultimate strength σ_u) were under consideration, only the curves reaching the ultimate strain have been utilised in the analysis; these curves are denoted Group II. Table 3 shows the number of experimental stress–strain curves considered in the different analyses for the studied stainless steel families.

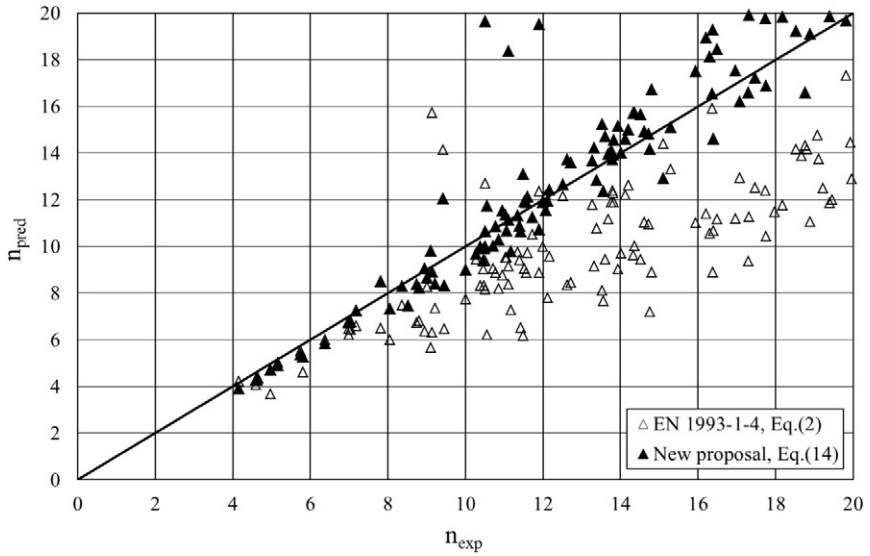

Fig. 10. Prediction of strain hardening parameter *n* for ferritic stainless steels.

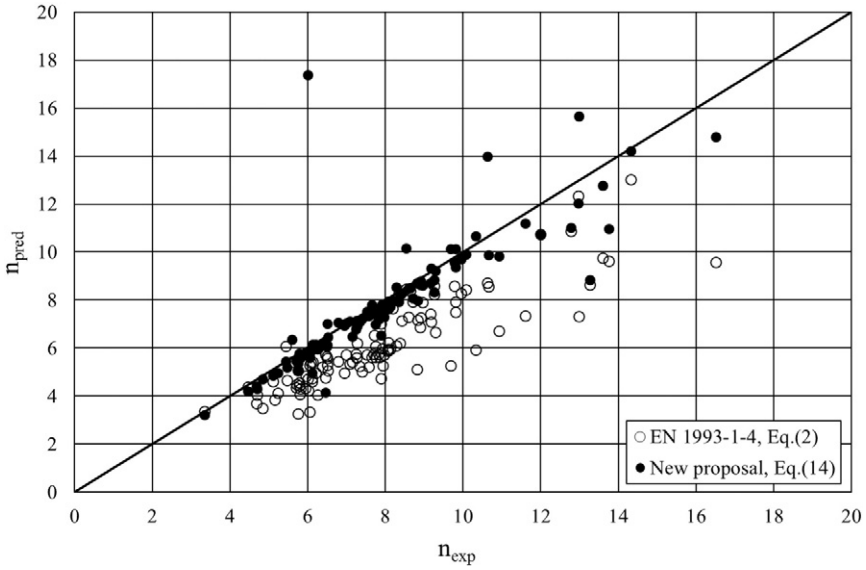

Fig. 11. Prediction of strain hardening parameter *n* for duplex and lean duplex stainless steels.

With the aim of simplifying the calculation of the material parameters from every analysed experimental stress–strain curve and moreover, carry out the complex calculation needed for the optimization of the strain hardening exponents *n* and *m*, a programme which automates all the required processes was developed. Although the key features of the programme are discussed in this paper, more extensive and detailed information can be found in Real et al. [4] and Westeel [35].

The programme first obtains the Young's modulus for each experimental curve from a linear regression analysis of a representative set of data. This data set has to be carefully defined, since the elastic modulus is sensitive to the range of data considered. Hence, the initial data recorded during the machine-coupon settlement, as well as any points on the nonlinear branch of the curves are removed. The proof stresses, including the 0.2% proof stress $\sigma_{0.2}$ which is conventionally used as the yield stress, corresponding to a plastic strain p σ_p are then obtained by determining the intersection point between a line with the same slope as the initial Young's modulus but passing through the offset strain p and the measured stress–strain curve. The ultimate strength σ_u and the corresponding ultimate strain ε_u are also captured.

Determination of the strain hardening exponents is carried out by a least square adjustment approach, providing values of *n* and *m* that closely match the experimental curves to the considered material model by minimizing the error between the two. A similar approach was employed by Afshan et al. [6]. Since the calculated values of the strain hardening parameters depend on the considered material model, assessment of two-stage models is presented in the next section in order to determine the most appropriate for further analysis.

Table 5
Prediction of strain hardening exponent *n* for different stainless steel families.

		n_{exp}/n_{pred} (Eq. (2))	n_{exp}/n_{pred} (Eq. (14))
Austenitic	Mean	1.19	1.02
	COV.	0.224	0.080
Ferritic	Mean	1.35	0.95
	COV.	0.171	0.133
Duplex and lean duplex	Mean	1.47	1.05
	COV.	1.301	0.146
All	Mean	1.28	1.01
	COV.	0.661	0.113

4.2. General assessment of two-stage models

As established in Section 2, different approaches are available for the modelling of stainless steel material behaviour. The two-stage models that can represent full stainless steel stress–strain curves up to σ_u are those of Mirambell and Real [7] and Rasmussen [8]. The main difference between these two models is the simplification that the latter considers, presented in Eq. (9), which assumes that the ultimate plastic strain in the second reference system ε^*_{up} is equal to the total ultimate strain ε_u, by neglecting the $\varepsilon_{0.2} + \frac{\sigma_u - \sigma_{0.2}}{E_{0.2}}$ term. This simplification is likely to be reasonable for the more ductile stainless steel grades (austenitic and duplex) where the neglected term is small compared to ε_u, which were originally studied by Rasmussen [8], but needs to be assessed for the less ductile ferritic grades, particularly if the material has been cold-worked. Table 4 evaluates the implications of the simplification

Table 6
Summary of measured strain hardening exponents (*n* and *m*) for Database I.

Family	Grade	Product type	RD/TD/45°	T/C	*n*	*m*
Austenitic	1.4301	Sheet	RD	T	10.2	2.2
		Sheet	RD	C	11.8	–
		Cold-formed	RD	T	7.9	3.7
		Cold-formed	RD	C	4.8	–
	1.4435	Sheet	RD	T	11.8	2.6
	1.4541	Sheet	RD	T	10.7	2.3
	1.4307	Sheet	RD	T	11.8	2.5
	1.4571	Cold-formed	RD	T	6.8	3.2
	1.4404	Cold-formed	RD	T	7.2	3.7
	1.4318	Cold-formed	RD	T	5.2	–
Ferritic	1.4016	Sheet	RD	T	13.6	3.0
		Sheet	TD	T	17.8	2.6
	1.4003	Sheet	RD	T	17.4	2.7
		Sheet	TD	T	16.9	2.6
		Cold-formed	RD	T	9.8	4.8
	1.4509	Sheet	RD	T	15.5	2.8
		Sheet	TD	T	21.6	2.9
		Cold-formed	RD	T	11.8	–
	1.4521	Sheet	RD	T	18.5	2.6
Duplex and lean duplex	1.4462	Sheet	RD	T	8.1	3.9
		Cold-formed	RD	T	6.9	3.9
	1.4162	Sheet	RD	T	9.6	3.5
		Sheet	TD	T	10.6	3.4
		Cold-formed	RD	T	8.3	4.7
		Sheet	RD	C	7.2	–
		Sheet	TD	C	7.9	–

Table 7
Codified and recommended values for strain hardening parameter *n*.

Family	Grade	RD/TD	T/C	Codified *n*			Recommended *n*
				EN 1993-1-4 [3]	AS/NZS-4673 [37]	SEI/ASCE-8 [38]	
Austenitic	1.4301	RD	T	6	7.5	8.3	7
	1.4301	RD	C	6	4.0	4.1	
	1.4435	RD	T	7	–	–	
	1.4541	RD	T	6	–	–	
	1.4307	RD	T	6	7.5	–	
	1.4571	RD	T	7	–	–	
	1.4404	RD	T	7	7.5	–	
	1.4318	RD	T	6	–	–	
	No. of curves:		367				
Ferritic	1.4016	RD	T	6	8.5	8.4	14
	1.4003	RD	T	7	9.0	–	
	1.4509	RD	T	–	–	–	
	1.4521	RD	T	–	11.0	–	
	No. of curves:		117				
	1.4016	TD	T	14	14.0	14.1	
	1.4003	TD	T	11	11.5	–	
	1.4509	TD	T	–	–	–	
	No. of curves:		32				
Duplex and lean duplex	1.4462	RD	T	5	5.5	–	8
	1.4162	RD	T	–	–	–	
	1.4162	RD	C	–	–	–	
	No. of curves:		92				
	1.4162	TD	T	–	–	–	
	1.4162	TD	C	–	–	–	
	No. of curves:		22				

defined in Eq. (9) for the different stainless steel families by presenting the mean, minimum and maximum values of the ratio of ultimate strains with and without the neglected term. Mean values of ultimate strain ε_u for the different stainless steel families are also presented.

Comparisons of the Mirambell–Real (MR) model and Rasmussen (R) model with measured stress–strain curves of austenitic and (cold-formed) ferritic stainless steel are shown in Figs. 7 and 8, respectively. The figures show that while the ultimate experimental stress and strain ($\sigma_{u,exp}$ and $\varepsilon_{u,exp}$) coincide precisely with the ultimate stress and strain $\varepsilon_{u,MR}$ in the case of Mirambell–Real model, this is not the case for the Rasmussen model. In the later model, the ultimate strain $\varepsilon_{u,R}$ will always be greater than the experimental values, and by a larger proportion of the full curve for the less ductile materials, as indicated in Table 4. However, both models may be seen to accurately capture the overall stress–strain response of the two materials, and the discrepancies associated with the approximation of ultimate strain in the Rasmussen model are restricted to the latter portion of the curves. It is therefore concluded that both models are applicable to all stainless steel grades. It may also be noted that if the Rasmussen model is curtailed at $\varepsilon_{u,exp}$ and the corresponding stress, which will be marginally below $\sigma_{u,exp}$, improved accuracy in the prediction of the ultimate region of the stress–strain response is achieved.

4.3. Analysis of first strain hardening exponent n

The accuracy of the classical expression proposed by Ramberg–Osgood [1] for the first strain hardening exponent *n*, as given by Eq. (2), is assessed herein. This constant is traditionally calculated by imposing that the analytical curve passes through the 0.01% and the 0.2% proof stresses. This is also the approach recommended in EN 1993-1-4. Different authors (Mirambell and Real [7], Rasmussen and Hancock [36], Real et al. [4] and Arrayago et al. [5]) have already

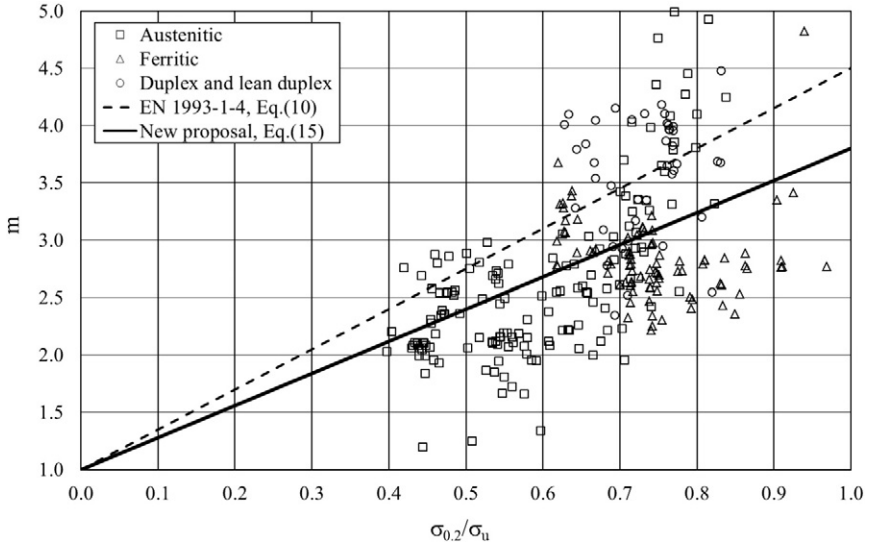

Fig. 12. Assessment of strain hardening parameter *m* for different stainless steel families.

Table 8
Assessment of strain hardening exponent m for different stainless steel families.

		EN1993-1-4, Annex C	Proposed
		m_{exp}/m_{pred} (Eq. (10))	m_{exp}/m_{pred} (Eq. (15))
Austenitic	Mean	0.84	0.98
	COV.	0.196	0.196
Ferritic	Mean	0.79	0.93
	COV.	0.153	0.150
Duplex and lean duplex	Mean	1.03	1.19
	COV.	0.264	0.148
All	Mean	0.85	1.00
	COV.	0.191	0.193

Table 9
Assessment of ultimate strength σ_u for different stainless steel families.

		$\sigma_{u,exp}/\sigma_{u,pred}$	
		Rasmussen [8]	Proposed
		Eq. (12a) for austenitic, duplex, lean duplex Eq. (12b) for ferritics	Eq. (12a) for austenitic, duplex, lean duplex Eq. (16) for ferritics
Austenitic	Mean	1.03	1.03
	COV.	0.126	0.126
Ferritic	Mean	1.41	0.97
	COV.	0.403	0.109
Duplex and lean duplex	Mean	0.98	0.98
	COV.	0.067	0.067

suggested that using the 0.05% proof stress instead of 0.01%, as given by Eq. (14), may provide a better representation of stainless steel experimental stress–strain curves.

$$n = \frac{\ln(4)}{\ln\left(\frac{\sigma_{0.2}}{\sigma_{0.05}}\right)} \tag{14}$$

Assessment of the two expressions (Eqs. (2) and (14)) for the determination of n is presented in Figs. 9–11 and Table 5, where comparisons with the values obtained from experimental curves are shown. The predicted values of n are referred to as n_{pred}, while those obtained from the experiments through the described least squares optimisation process are denoted n_{exp}. The results clearly demonstrate that Eq. (14) provides considerably more accurate predictions of the measured n values than Eq. (2), which is currently specified in Annex C of EN 1993-1-4. It is therefore recommended that EN1993-1-4 is modified to reflect this finding and that authors report the 0.05% proof stress $\sigma_{0.05}$ from their experimental studies in the future.

The mean values of the measured strain hardening parameters (n and m) for different stainless steel grades, section types and testing directions are presented in Table 6. The lowest n values were obtained for the austenitic and duplex grades, reflecting the more rounded stress–strain behaviour, while the ferritic grades exhibited the sharpest yield response and therefore the highest n values. The results also showed that the n values generally decrease as the level of cold-work increases, and that higher n values arose for material tested in the transverse direction than the longitudinal direction.

As noted earlier, in addition to providing formulae for the determination of n from experimental σ–ε data, the various stainless steel design Standards (EN 1993-1-4 [3], AS/NZS 4673 [37] and SEI/ASCE-8-02 [38]) also provide numeric values for n for the different stainless steel grades. Differentiation is sometimes made between the material type (annealed or cold-formed), orientation of loading (rolling direction or transverse direction) and sense of loading (tension and compression). While EN 1993-1-4 only distinguishes between transverse or longitudinal directions, the Australian/New Zealand standard considers both the orientation of loading (transverse or longitudinal) and the sense of loading (tension or compression). The North American specification considers not only the loading sense and orientation, but also the material's level of cold-work. Following careful analysis of the collated n values, recommendations for values of the n parameter are presented in Table 7, where the number of curves from which the recommended values have been derived is also provided. These recommended values are close to those proposed by Afshan et al. [6], but benefit from a larger database of results, including all those considered by [6]. Note that the n values proposed herein are slightly higher than those recommended by Afshan et al. [6]. This is attributed to the different data sets that were analysed and the fact that the data set considered herein included a higher proportion of sheet material. This is relevant because cold-working of the sheet material, which would be experienced in the cold-forming of structural sections, produces a slightly more rounded stress–strain response i.e., lower n values.

It should also be noted that it is proposed that no distinction is made between loading directions (transverse or longitudinal), sense of loading (tension or compression) or cold-worked level in assigning the values of n. This is for the following reasons: (1) simplicity, (2) there are insufficient data to enable a meaningful distinction to be drawn for many grades, (3) influence of the above parameters is generally

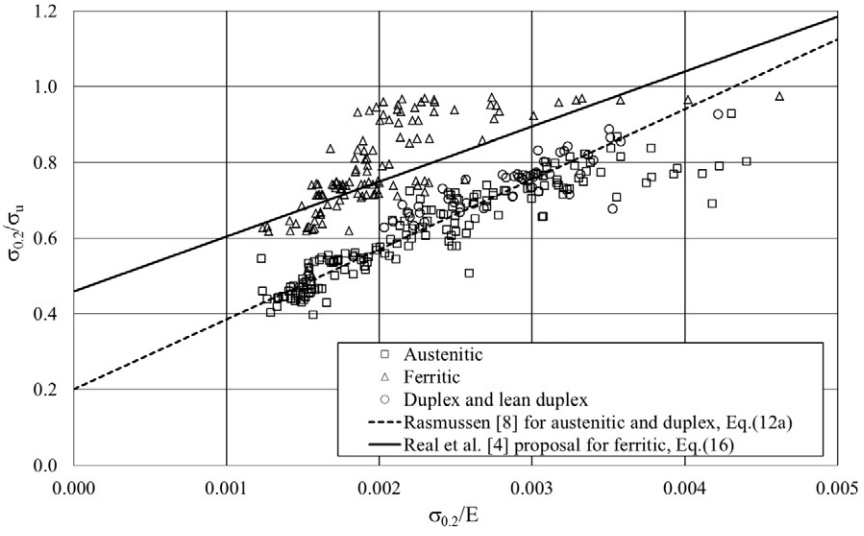

Fig. 13. Assessment of ultimate strength σ_u for different stainless steel families.

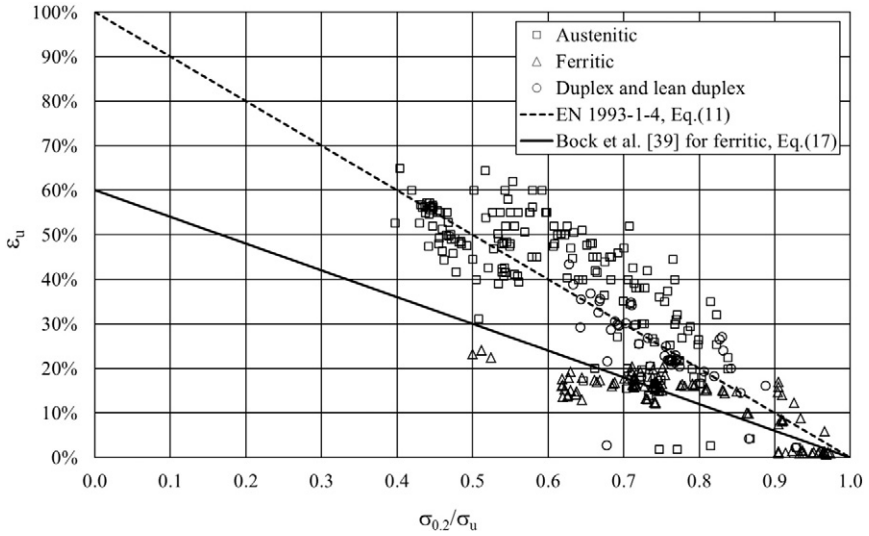

Fig. 14. Assessment of ultimate strain ε_u for different stainless steel families.

relatively small in terms of the effect on the shape of the stress–strain curve, (4) a designer will not typically know whether the material will be orientated in the transverse or longitudinal direction, (5) the same structural element can be subjected to tension and compression depending on the load case under consideration, and (6) the level of cold-work (i.e., the amount of plastic strain to which the material has been subjected) will depend on the section geometry, the forming process and so on.

4.4. Analysis of second strain hardening exponent m

Eq. (10) is provided in Annex C of EN 1993-1-4 for the determination of the second strain hardening exponent *m*. Recent studies involving the examination of austenitic and ferritic stainless steel stress–strain curves (Real et al. [4]; Arrayago et al. [5]) found that this expression provides higher values for the second strain hardening exponent *m* than those obtained from curve fitting. This issue is explored further herein, utilising the assembled database. Fig. 12 shows the experimental strain hardening exponents (obtained through the described curve fitting process) plotted against $\sigma_{0.2}/\sigma_u$ for the different stainless steel grades. Table 8 presents the mean experimental to predicted ratios of the second strain hardening parameters m_{exp}/m_{pred} for all the studied stainless steel stress–strain curves that reached the ultimate strain, referred to as Group II in Table 3. The mean m_{exp}/m_{pred} ratios are low for the majority of the analysed data, particularly the austenitic and ferritic grades. A revised expression, given by Eq. (15), was therefore proposed for all stainless steel grades, based on least squares regression.

$$m = 1 + 2.8\frac{\sigma_{0.2}}{\sigma_u} \tag{15}$$

Overall, the new proposal provides more accurate predictions for the second strain hardening parameter *m* than the existing formula (Eq. (10)) and is therefore recommended for code inclusion.

Table 10
Assessment of ultimate strain ε_u for different stainless steel families.

		$\varepsilon_{u,exp}/\varepsilon_{u,pred}$	
		EN1993-1-4, Annex C	Proposed
		Eq. (11)	Eq. (11) for austenitic, duplex, lean duplex Eq. (17) for ferritics
Austenitic	Mean	1.09	1.09
	COV.	0.280	0.280
Ferritic	Mean	0.59	0.98
	COV.	0.565	0.565
Duplex and lean duplex	Mean	0.96	0.96
	COV.	0.275	0.275

4.5. Analysis of σ_u

Rasmussen [8] developed an expression to predict σ_u in terms of two of the basic Ramberg–Osgood parameters, $\sigma_{0.2}$ and E. The accuracy of this expression is assessed herein against the assembled test data, as shown in Fig. 13, where $\sigma_{0.2}/\sigma_u$ ratios have been plotted against $\sigma_{0.2}$/E for the Group II data. The experimental results have been compared to different predictive models: Eq. (12a) proposed by Rasmussen [8] for the austenitic and duplex grades and Eq. (16) proposed by Real et al. [4] for the ferritic grades.

$$\frac{\sigma_{0.2}}{\sigma_u} = 0.46 + 145\frac{\sigma_{0.2}}{E} \tag{16}$$

Fig. 13 and Table 9 show that the original expression for the determination of σ_u for austenitic, duplex and lean duplex stainless steels proposed by Rasmussen [8] provides very good predictions of the assembled data set, so the validity of Eq. (12a) is confirmed. However, for ferritic stainless steels, Eq. (12b), which was proposed by Rasmussen for all stainless steel grades, provides inaccurate results. The accuracy of the revised expression proposed by Real et al. [4] for the ferritic grades has been confirmed by the experimental data analysed in Arrayago et al. [5] and the additional data studied herein.

4.6. Analysis of ε_u

Assessment of the predictive expressions for ultimate strain is presented in Fig. 14, where the experimental ultimate strain ε_u is plotted against $\sigma_{0.2}/\sigma_u$ ratios for data from 171 austenitic, 94 ferritic and 50 duplex and lean duplex stainless steel tensile tests. Together with the experimental data, the expression for the determination of the ultimate strain provided in Annex C of EN 1993-1-4, given by Eq. (11), is also plotted. From Fig. 14, this expression may be seen to provide very good predictions for the austenitic, duplex and lean duplex materials,

Table 11
Summary of additional experimental results (Database II).

Family	Grade	No. of curves	Product type	RD/TD/45°	T/C	Thickness range (mm)	Reference
Austenitic	1.4301	4	Cold-formed	RD, TD, 45	T, C	2	Becque and Rasmussen [40]
	1.4301	6	Cold-formed	RD, TD, 45	T, C	8.5	Becque and Rasmussen [41]
	1.4301	7	Cold-formed	RD	T, C	1.2–2	Niu and Rasmussen [42]
	1.4301, 1.4435	139	Sheets	RD, TD	T, C	2–10	Rasmussen [43]
	1.4301	8	Cold-formed	RD	T, C	3	Rasmussen and Hancock [44]
	1.4301	2	Cold-formed	RD	T	3	Rasmussen and Hasham [45]
	1.4301	3	Cold-formed	RD	T	3	Rasmussen and Young [46]
	1.4301	2	Cold-formed	RD	T	5	Yousuf et al. [47]
	1.4301	16	Cold-formed	RD	T	2–3	Fan et al. [48]
	1.4301	12	Cold-formed	RD	T	1.2–4.8	Uy et al. [49]
	1.4301	3	Cold-formed	RD	T	5	Han et al. [50]
	1.4401	6	Cold-formed	RD	T	2–3	Theofanous et al. [51]
	1.4301	2	Cold-formed	RD	T	2	Liu and Young [52]
Ferritic	1.4003	18	Cold-formed	RD, TD, 45	T, C	1–2	Becque and Rasmussen [40]
	404	6	Cold-formed	RD, TD, 45	T, C	1.2	Becque and Rasmussen [41]
	1.4003, 1.4016	8	Cold-formed	RD, TD	T, C	1.2–2	Lecce and Rasmussen [53]
	1.4521	7	Cold-formed	RD	T, C	1.2–2	Niu and Rasmussen [42]
	1.4003	12	Sheet	RD	T	2–10	Rasmussen [43]
	1.4003	2	Cold-formed	RD	T	3	Tondini et al. [54]
	1.4003	5	Cold-formed	RD	T	3–4	Islam and Young [55]
	1.4509	21	Cold-formed	RD	T	1–3	Talja and Hradil [30]
Duplex and lean duplex	1.4462	93	Sheets	RD, TD	T, C	2–12	Rasmussen [43]
	1.4462	6	Sheets	RD	T, C	3	Rasmussen et al. [56]
	HSD	8	Cold-formed	RD	T	1.5–3	Ellobody and Young [57]
	1.4462	5	Cold-formed	RD	T	3–6	Ellobody and Young [58]
	HSD	4	Cold-formed	RD	T	2–3	Young and Lui [59]
	1.4162	7	Cold-formed	RD	T, C	1.5	Niu and Rasmussen [42]

RD: rolling direction, TD: transverse direction, 45°: 45° from the rolling direction.
T: tension, C: compression.
HSD: high strength duplex.

so its accuracy is confirmed for these stainless steel families. However, as found in previous material modelling studies (Real et al. [4]; Arrayago et al. [5]; Bock et al. [39]), ferritic stainless steels exhibit less ductile behaviour than the austenitic and duplex grades, and Eq. (11) yields unconservative predictions of ε_u. Bock et al. [39] conducted a detailed study of the prediction of ε_u for ferritic stainless steel, and proposed a revised expression, described by Eq. (17). As shown in Fig. 14 and Table 10, Eq. (17) also provides good predictions for the ferritic stainless steel data set assembled herein.

$$\varepsilon_u = 0.6\left(1-\frac{\sigma_{0.2}}{\sigma_u}\right) \tag{17}$$

5. Additional validation and summary of proposals

5.1. Additional validation of the proposals

This section presents an evaluation of the proposed equations through an independent experimental database gathered from the literature. In addition to the experimental results summarised in Table 2, which were available to the authors to analyse in the form of raw data, further results reported and analysed by others were also collected. This additional collection of results, referred to as Database II, is presented in Table 11 and consists of more than 400 tests. The results in this second database show a higher dispersion than Database I since the methodology for the calculation of the parameters will differ slightly between authors. The database comprises tests on different stainless steel families, cross-sectional shapes, thicknesses and testing directions. Not all material parameters were reported for all specimens, so some expressions could only be evaluated against a sub-set of the database.

Tables 12 to 14 compare the mean experimental to predicted ratios for the experimental results of Database II for m, σ_u and ε_u respectively, where the accuracy of the recommended expressions is assessed.

The results show that the prediction of the key material parameters is more accurate when the proposals (when relevant) are considered, as the mean experimental to predicted ratios get closer to the unity, although the scatter of the data is generally maintained, in line with the dispersion presented by the analysed data. The new expressions proposed in Section 4 are found to accurately predict the material parameters reported by other authors: the strain hardening exponent m for austenitic and ferritic stainless steels and the ultimate strength and

Table 12
Assessment of the second strain hardening exponent m for different stainless steel families for Database II.

		EN1993-1-4, Annex C	Proposed
		m_{exp}/m_{pred} (Eq. (10))	m_{exp}/m_{pred} (Eq. (15))
Austenitic	Mean	0.92	1.06
	COV.	0.186	0.190
Ferritic	Mean	0.67	0.78
	COV.	0.458	0.456
Duplex and lean duplex	Mean	–	–
	COV.		

Table 13
Assessment of the ultimate strength σ_u for different stainless steel families for Database II.

		$\sigma_{u,exp}/\sigma_{u,pred}$	
		Rasmussen [8]	Proposed
		Eq. (12a) for austenitic, duplex, lean duplex Eq. (12b) for ferritics	Eq. (12a) for austenitic, duplex, lean duplex Eq. (16) for ferritics
Austenitic	Mean	1.03	1.03
	COV.	0.097	0.097
Ferritic	Mean	1.28	0.98
	COV.	0.620	0.093
Duplex and lean duplex	Mean	0.99	0.99
	COV.	0.064	0.064

Table 14
Assessment of the ultimate strain ε_u for different stainless steel families for Database II.

		$\varepsilon_{u,exp}/\varepsilon_{u,pred}$	
		EN1993-1-4, Annex C	Proposed
		Eq. (11)	Eq. (11) for austenitic, duplex, lean duplex Eq. (17) for ferritics
Austenitic	Mean	1.02	1.02
	COV.	0.253	0.253
Ferritic	Mean	0.71	1.06
	COV.	0.335	0.237
Duplex and lean duplex	Mean	1.04	1.04
	COV.	0.298	0.298

strain for ferritics. The original expressions seem to correctly estimate the experimental values of m, σ_u and ε_u for the other grades.

5.2. Summary of proposals

Based on the described analyses, the proposed predictive expressions and the recommended modifications to made to Annex C of EN1993-1-4 are summarised as follows:

$$n = \frac{\ln(4)}{\ln\left(\frac{\sigma_{0.2}}{\sigma_{0.05}}\right)} \quad \text{for all grades} \qquad \text{(Eq. (14))}$$

$$m = 1 + 2.8\frac{\sigma_{0.2}}{\sigma_u} \quad \text{for all grades} \qquad \text{(Eq. (15))}$$

$$\frac{\sigma_{0.2}}{\sigma_u} = \begin{cases} 0.20 + 185\frac{\sigma_{0.2}}{E} & \text{for austenitic, duplex and lean duplex} \quad \text{(Eq. (12a))} \\ 0.46 + 145\frac{\sigma_{0.2}}{E} & \text{for ferritic grades} \quad \text{(Eq. (16))} \end{cases}$$

$$\varepsilon_u = \begin{cases} 1 - \frac{\sigma_{0.2}}{\sigma_u} & \text{for austenitic, duplex and lean duplex} \quad \text{((Eq. (11))} \\ 0.6\left(1 - \frac{\sigma_{0.2}}{\sigma_u}\right) & \text{for ferritic grades} \quad \text{(Eq. (17))} \end{cases}.$$

Additionally, the revised values for the first strain hardening parameter n, presented in Table 7, are recommended for inclusion in EN1993-1-4. The numeric values of Young's modulus for stainless steel proposed by Afshan et al. [6] are also recommended herein.

6. Conclusions

A comprehensive study into the nonlinear stress–strain response of stainless steel alloys and the modelling thereof is presented in this paper. A total of over 600 experimental stress–strain curves, including austenitic, ferritic and duplex grades has been collected and analysed. The collected data have been used for the assessment of existing two-stage material models and the expressions for the prediction of the key material parameters. The material model proposed by Rasmussen [8], and currently included in Annex C of EN 1993-1-4, was found to accurately represent the measured stress–strain curves for the different stainless steel grades and material types, including ferritic stainless steels for which the model had not previously been fully verified.

Based on the assembled data set, values and predictive expressions for the key material parameters of the Rasmussen model were re-evaluated. A revised predictive equation and revised numeric values for the strain hardening parameter n have been recommended for all stainless steel families. A new expression for the prediction of the second strain hardening parameter m for all stainless steel grades has also been proposed. Finally, revised predictive expressions for ultimate tensile stress and strain for ferritic stainless steels have been proposed. It is recommended that the above proposals are incorporated into future revisions of EN 1993-1-4.

Acknowledgements

The tested coupons presented in this work were provided by Acerinox, and the experiments were funded by the Ministerio de Economía y Competitividad (Spain) under the Project BIA 2012-36373. The first author would like to acknowledge the financial support given by UPC. The authors would also like to recognize all the people and institutions that have provided the experimental curves for this research, the European Community's Research Fund for Coal and Steel (RFCS) under Grant Agreement No. RFSR-CT-2010-00026, and the Ministerio de Ciencia e Innovación (Spain) under the Project BIA2010-11876-E "Acciones complementarias". Finally, the authors would also like to thank all those who assisted during the tensile tests, especially Francisco Gonzalez.

References

[1] W. Ramberg, W.R. Osgood, Description of stress–strain curves by three parameters, Technical Note No. 902, National Advisory Committee for Aeronautics, Washington, D.C., USA, 1943 (1943).
[2] H.N. Hill, Determination of stress–strain relations from "offset" yield strength values, Technical Note No. 927, 1944 (1944).
[3] EN, 1993-1-4, Eurocode 3: Design of Steel Structures — Part 1–4: General Rules — Supplementary Rules for Stainless Steels, European Committee for Standardization, Brussels (2006).
[4] E. Real, I. Arrayago, E. Mirambell, R. Westeel, Comparative study of analytical expressions for the modelling of stainless steel behaviour, Thin-Walled Struct. 83 (2014) 2–11.
[5] I. Arrayago, E. Real, E. Mirambell, et al., Constitutive equations for stainless steels: experimental tests and new proposal, Proceedings of the Fifth International Conference on Structural Engineering, Mechanics and Computation. Cape Town, South Africa 2013, pp. 1435–1440.
[6] S. Afshan, B. Rossi, L. Gardner, Strength enhancements in cold-formed structural sections — part I: material testing, J. Constr. Steel Res. 83 (2013) 177–188.
[7] E. Mirambell, E. Real, On the calculation of deflections in structural stainless steel beams: an experimental and numerical investigation, J. Constr. Steel Res. 54 (4) (2000) 109–133.
[8] K.J.R. Rasmussen, Full-range stress–strain curves for stainless steel alloys, J. Constr. Steel Res. 59 (1) (2003) 47–61.
[9] L. Gardner, M. Ashraf, Structural design for non-linear metallic materials, Eng. Struct. 28 (6) (2006) 926–934.
[10] L. Gardner, A. Insausti, K.T. Ng, M. Ashraf, Elevated temperature material properties of stainless steel alloys, J. Constr. Steel Res. 66 (5) (2010) 634–647.
[11] W.M. Quach, J.G. Teng, K.F. Chung, Three-stage full-range stress–strain model for stainless steels, J. Struct. Eng. ASCE 134 (9) (2008) 1518–1527.
[12] P. Hradil, A. Talja, E. Real, E. Mirambell, B. Rossi, Generalized multistage mechanical model for nonlinear metallic materials, Thin-Walled Struct. 63 (2013) 63–69.
[13] EN ISO 6892-1. 2009, Metallic materials — tensile testing, Part 1: Method of Test at Room Temperature. European Committee for Standardization (CEN), Brussels, 2009 (2009).
[14] Y. Huang, B. Young, The art of coupon tests, J. Constr. Steel Res. 96 (2014) 159–175.
[15] I. Estrada, E. Real, E. Mirambell, Stainless steel girders longitudinally stiffened: behaviour in shear, Experimental and numerical analysis, Eurosteel 2005, 4th European Conference on Steel and Composite Structures. Maastrich, Netherlands, 2005, 1.4 2005, pp. 215–220.
[16] E. Real, E. Mirambell, I. Estrada, Shear response of stainless steel plate girders, Eng. Struct. 29 (7) (2007) 1626–1640.
[17] K.H. Nip, L. Gardner, A.Y. Elghazouli, Cyclic testing and numerical modelling of carbon steel and stainless steel tubular bracing members, Eng. Struct. 32 (2) (2010) 424–441.
[18] M. Xu, M. Szalyga, Comparative Investigations on the Load-bearing Behaviour of Single Lap Joints with Bolts Stressed in Shear and Bearing-experimental and Simulation, University of Duisburg-Essen, Institute for Metal and Lightweight Structures, 2011 (Master Project, 2011).
[19] L. Gardner, A New Approach to Structural Stainless Steel Design(Doctoral Thesis) Imperial College London, 2002.
[20] L. Gardner, D. Nethercot, Experiments on stainless steel hollow sections — part 1: material and cross-sectional behaviour, J. Constr. Steel Res. 60 (9) (2004) 1291–1318.
[21] A. Talja, Development of the use of stainless steel in construction, Test Report on Welded I and CHS Beams, Columns and Beam–Columns. WP 3.1, 3.2 and 3.3, Final ReportVTT Technical Research Centre of Finland, 1997 (December 1997).
[22] A. Talja, Development of the use of stainless steel in construction, Test report on Z Sections Restrained by Sheeting. WP 3.1, 3.2 and 3.3, Final ReportVTT Technical Research Centre of Finland, 1997 (August 1997).

[23] A. Talja, Development of the use of stainless steel in construction, Test Report on Sheeting. WP 3.1, 3.2 and 3.3, Final ReportVTT Technical Research Centre of Finland, 1997 (August 1997).
[24] A. Talja, Structural design of cold-worked austenitic stainless steel, Test Results of RHS, Top-hat and Sheeting Profiles. WP 3.1, 3.2 and 3.3, Final ReportVTT Technical Research Centre of Finland, 2002 (December 2002).
[25] F. Zhou, B. Young, Experimental and numerical investigations of cold-formed stainless steel tubular sections subjected to concentrated bearing load, J. Constr. Steel Res. 63 (2007) 1452–1466.
[26] T. Manninen, Structural applications of ferritic stainless steels (SAFSS): WP1 end-user requirements and material performance, Task 1.3 Characterization of stress–strain behaviour: Technical Specifications for Room-Temperature: Tensile and Compression Testing, 2011.
[27] E. Real, E. Mirambell, I. Arrayago, F. Marimon, Structural application of ferritic stainless steels (SAFSS): WP3: structural and thermal performance of steel-concrete composite floor systems, Task 3.2: Decking Tests in the Construction Stage. Internal Report, 2012.
[28] S. Afshan, L. Gardner, Experimental study of cold-formed ferritic stainless steel hollow sections, J. Struct. Eng. ASCE 139 (5) (2013) 717–728.
[29] B. Rossi, Mechanical behaviour of ferritic grade 3Cr12 stainless steel. Part 1: experimental investigations, Thin-Walled Struct. 48 (2010) 553–560.
[30] A. Talja, P. Hradil, Structural performance of steel members: model calibration tests, SAFSSWP2 Internal Report, 2011.
[31] M. Theofanous, L. Gardner, Experimental and numerical studies of lean duplex stainless steel beams, J. Constr. Steel Res. 66 (2010) 816–825.
[32] N. Saliba, L. Gardner, Experimental study of the shear response of lean duplex stainless steel plate girders, Eng. Struct. 46 (2013) 375–391.
[33] N. Saliba, L. Gardner, Cross-section stability of lean duplex stainless steel welded I-sections, J. Constr. Steel Res. 80 (2013) 1–14.
[34] Y. Huang, B. Young, Material properties of cold-formed lean duplex stainless steel sections, Thin-Walled Struct. 54 (2012) 72–81.
[35] R. Westeel, Análisis comparativo de expresiones analíticas para modelizar el comportamiento tenso-deformacional no lineal del acero inoxidable, Tesina de especialidad. , ETSECCPB, Universitat Politècnica de Catalunya, 2012.
[36] K.J.R. Rasmussen, G.J. Hancock, Design of cold-formed stainless steel tubular members II: beams, J. Struct. Eng. ASCE 119 (8) (1993) 2368–2386.
[37] AS/NZS 4673, Cold-formed Stainless Steel Structures, Standards Australia, Sydney, 2001 (2001).
[38] SEI/ASCE 8-02, Specification for the Design of Cold-formed Stainless Steel Structural Members, American Society of Civil Engineers (ASCE), Reston, 2002 (2002).
[39] M. Bock, L. Gardner, E. Real, Material and local buckling response of ferritic stainless steel sections, Thin-Walled Struct. 89 (2015) 131–141.
[40] J. Becque, K.J.R. Rasmussen, Experimental investigation of local–overall interaction buckling of stainless steel lipped channel columns, J. Constr. Steel Res. 65 (2009) 1677–1684.
[41] J. Becque, K.J.R. Rasmussen, Experimental investigation of the interaction of local and overall buckling of stainless steel I-columns, J. Struct. Eng. ASCE 135 (11) (2009) 1340–1348.
[42] S. Niu, K.J.R. Rasmussen, F. Fan, Distortional–global interaction buckling of stainless steel C-beams: part I: experimental investigation, J. Constr. Steel Res. 96 (2014) 127–139.
[43] K.J.R. Rasmussen, Full-range stress–strain curves for stainless steel alloys, Research Report No. R811, Department of Civil Engineering. The University of Sydney, 2001.
[44] K.J.R. Rasmussen, G.J. Hancock, Design of cold-formed stainless steel tubular members. I: columns, J. Struct. Eng. ASCE 119 (8) (1993) 2349–2367.
[45] K.J.R. Rasmussen, A.S. Hasham, Tests of X- and K-joints in CHS stainless steel tubes, J. Struct. Eng. ASCE 127 (10) (2001) 1183–1189.
[46] K.J.R. Rasmussen, B. Young, Tests of X- and K-joints in SHS stainless steel tubes, J. Struct. Eng. ASCE 127 (10) (2001) 1173–1182.
[47] M. Yousuf, B. Uy, Z. Tao, A. Remennikov, J.Y.R. Liew, Transverse impact resistance of hollow and concrete filled stainless steel columns, J. Constr. Steel Res. 82 (2013) 177–189.
[48] S. Fan, F. Liu, B. Zheng, G. Shu, Y. Tao, Experimental study on bearing capacity of stainless steel lipped C section stub columns, Thin-Walled Struct. 83 (2014) 70–84.
[49] B. Uy, Z. Tao, L.H. Han, Behaviour of short and slender concrete-filled stainless steel tubular columns, J. Constr. Steel Res. 67 (2011) 360–378.
[50] L.H. Han, F. Chen, F.Y. Liao, Z. Tao, B. Uy, Fire performance of concrete filled stainless steel tubular columns, Eng. Struct. 56 (2013) 165–181.
[51] M. Theofanous, T.M. Chan, L. Gardner, Structural response of stainless steel oval hollow section compression members, Eng. Struct. 31 (2009) 922–934.
[52] Y. Liu, B. Young, Buckling of stainless steel square hollow section compression members, J. Constr. Steel Res. 59 (2003) 165–177.
[53] M. Lecce, K.J.R. Rasmussen, Distortional buckling of cold-formed stainless steel sections: experimental investigation, J. Struct. Eng. ASCE 132 (4) (2006) 497–504.
[54] N. Tondini, B. Rossi, J.M. Franssen, Experimental investigation on ferritic stainless steel columns in fire, Fire Saf. J. 62 (2013) 238–248.
[55] S.M.Z. Islam, B. Young, Ferritic stainless steel tubular members strengthened with high modulus CFRP plate subjected to web crippling, J. Constr. Steel Res. 77 (2012) 107–118.
[56] K.J.R. Rasmussen, T. Burns, P. Bezkorovainy, M.R. Bambach, Numerical modelling of stainless steel plates in compression, J. Constr. Steel Res. 59 (2003) 1345–1362.
[57] E. Ellobody, B. Young, Structural performance of cold-formed high strength stainless steel columns, J. Constr. Steel Res. 61 (2005) 1631–1649.
[58] E. Ellobody, B. Young, Experimental investigation of concrete-filled cold-formed high strength stainless steel tube columns, J. Constr. Steel Res. 62 (2006) 484–492.
[59] B. Young, W.M. Lui, Tests of cold-formed high strength stainless steel compression members, Thin-Walled Struct. 44 (2006) 224–234.